

Article

Effect of Process Parameters on Spinning Force and Forming Quality of Deep Cylinder Parts in Multi-Pass Spinning Process

Libo Li ^{1,2,†}, Siyuan Chen ^{3,4,†}, Qinying Lu ^{3,4}, Xuedao Shu ^{3,4,*} , Jun Zhang ^{1,2} and Weiwei Shen ^{1,2}

¹ Healthy & Intelligent Kitchen Engineering Research Center of Zhejiang Province, Ningbo 315336, China

² Ningbo Fotile Kitchen Ware Company, Ningbo 315336, China

³ Faculty of Mechanical Engineering and Mechanics, Ningbo University, Ningbo 315211, China

⁴ Zhejiang Provincial Key Laboratory of Part Rolling Technology, Ningbo 315211, China

* Correspondence: shuxuedao@nbu.edu.cn

† These authors contributed equally to this work.

Abstract: In this paper, based on MSC Simufact.Forming v16.0 simulation software, the process parameters in the multi-pass spinning production of deep cylinders with a large diameter–thickness ratio are optimized, and the ten-pass spinning process of a deep cylinder with a diameter of 500 mm, thickness of 2 mm and depth of 700 mm is realized. By controlling the four process parameters of mandrel speed, feed rate, spinning wheel fillet radius and spinning wheel angle of attack, the influence of the four process parameters on the spinning force and the wall thickness deviation of the formed workpiece is studied. The results show that the radial spinning force and tangential spinning force are at their minimum when the mandrel speed, feed rate, spinning wheel fillet radius and spinning wheel angle of attack are 500 rpm, 1 mm/rev, 6 mm and 35°, respectively. At these setup conditions, the spinning efficiency is the highest and the workpiece is not prone to defects. The wall thickness deviation of the workpiece will decrease with the increase in the mandrel speed; with the increase in the feed rate, the radius of the round corner and spinning wheel angle of attack, the wall thickness deviation increases first and then decreases.



Citation: Li, L.; Chen, S.; Lu, Q.; Shu, X.; Zhang, J.; Shen, W. Effect of Process Parameters on Spinning Force and Forming Quality of Deep Cylinder Parts in Multi-Pass Spinning Process. *Metals* **2023**, *13*, 620. <https://doi.org/10.3390/met13030620>

Academic Editor: Ricardo J. Alves de Sousa

Received: 22 February 2023

Revised: 14 March 2023

Accepted: 15 March 2023

Published: 20 March 2023



Copyright: © 2023 by the authors. Licensee MDPI, Basel, Switzerland. This article is an open access article distributed under the terms and conditions of the Creative Commons Attribution (CC BY) license (<https://creativecommons.org/licenses/by/4.0/>).

Keywords: deep cylinder parts; spinning force; wall thickness deviation; multi-pass spinning

1. Introduction

Spinning is an advanced process that integrates forging, extrusion, stretching, bending and other process characteristics [1], which is widely used in national defense, civil industry and other fields in China. It has the advantages of a high material utilization rate, short production cycle, simple equipment and high-quality products [2], which can easily manufacture various symmetrical and seamless rotary parts. The production of deep cylinder parts generally adopts the spinning process. The forming mechanism of this kind of workpiece is complex, and it often needs to be gradually formed through multiple steps. For the study of deep cylindrical parts, Lu [3] et al. used the finite element analysis method to numerically simulate the spinning process of aluminum alloy cylindrical parts, and analyzed the three stages of spinning force change during the spinning process. Wang [4] predicted that the spinning damage accumulation of cylindrical parts mainly occurred in the metal uplift area through the damage model. Shi [5] used ABAQUS/Explicit software to simulate the stress state of the material and the distribution of the wall thickness of the workpiece in the circumferential direction in the multi-pass drawing of the cylindrical part. Based on Simufact finite element software, Li [6] explored the influence of the number of rollers on the forming quality of cylindrical parts. Zeng [7] found that the most uniform thickness of the spinning parts was obtained using the roller trace of convex and concave curves with round trip feed and no-pass foil advancing. When adopting this kind of roller trajectory, the larger the roller installation angle and feed ratio, the easier the workpiece wrinkles. Based on the finite element analysis software ANSYS/LS-DYNA, Mei [8] obtained

the spinning force and stress-strain law of aluminum alloy cylindrical parts under different process parameters. Taking the inner diameter deviation and wall thickness deviation as the evaluation indexes, Zhang et al. [9] studied the influence of the thinning rate, feed rate, blank die gap and mandrel speed on the thin-walled cylindrical parts with a large diameter-thickness ratio.

Multi-pass spinning is mostly used for deep cylinder parts, that is, the same blank is processed by the multi-stage spinning trajectory to obtain the target shape parts. Compared with single-pass spinning, the spinning trajectory is more complex, the limit drawing ratio is larger and the residual stress on the surface will also decrease [10]. Ma [11] studied the influence of linear trajectory, involute trajectory and Bessel curve trajectory on spinning formation by using unidirectional and reciprocal multi-pass spinning processing modes. Pan [12] et al. found that the wall thickness thinning experienced two stages of shear thinning and tension thinning during multi-pass spinning, and the severe thinning area was located behind the spinning wheel. Li [13] provided stress and thickness information for the design of the motion path of the spinning wheel through finite element simulation, and provided a reference for the selection of the distance from the starting point of the spinning wheel in the opposite direction to the edge position. Wang et al. [14] studied the influence of different curve trajectories on stress-strain and wall thickness distribution after the first positive rotation and the second reverse rotation through experiments and finite element simulation technology. Based on the equidistant multi-pass spinning trajectory planning method, Chen [15] provided the generation method of the spinning asymptote trajectory, so as to determine the starting point and end point of the spinning trajectory.

The spinning forming quality of deep cylinder parts is affected by the interaction of many factors, such as rotation speed, thinning rate, spinning gap, roller feed rate, roller fillet radius and roller installation angle, which makes it easy to produce defects such as instability wrinkling, tensile fracture and surface scratch indentation in the forming process. The prediction ability of the traditional weakest link can be improved by the surface factor and size sensitivity factor [16]. At the same time, the work hardening of the metal can demonstrate the dislocation substructure, explore the strain hardening mechanism [17], and reduce the generation of defects during processing. Han [18] found that in the process of spinning deep drawings of cylindrical parts, with the increase in the feed rate, the wall thickness of the cylinder wall will increase as a whole, but the larger the feed rate, the less obvious the relationship with the wall thickness. Based on Simufact, He et al. [19] explored the influence of friction coefficients on the forming accuracy of the workpiece in multi-pass thinning drawing. Li et al. [20] studied the influence of process parameters on the wall thickness, outer diameter and forming performance of the workpiece by a single-pass deep drawing spinning test. It was found that the larger feed ratio caused wrinkling and cracking of the workpiece more easily. Ebrahimi [21] studied the influence of feed rate, mandrel speed and thinning rate on the surface quality and geometric accuracy of the forming tube. Molladavoudi [22] summarized the influence of different wall thickness reductions on the quality of the product by spinning aluminum alloys on the modified CNC lathe. Wang [23] analyzed the influence of process parameters, such as the pass thinning rate, feed ratio, roller forming angle and roller fillet radius, on the roundness, straightness and wall thickness difference of thin-walled cylindrical spinning parts. Dahms [24] studied the influence of feed rate and rotational speed on the tangential and radial residual stress of the workpiece in the spinning process through experimental design. The numerical simulation of single-pass deep drawing spinning of a DP600 high-strength steel plate was carried out by Du [25]. The influence of the feed ratio of the roller, the fillet radius of the roller and the relative gap between the roller and the mandrel on the uniformity, straightness and roundness of the wall thickness distribution of the spinning parts was obtained. Gao [26] and Tang [27] used Simufact to study the influence of different process parameters on the accuracy of strong hot spinning.

The forming of deep cylinder parts needs to go through multi-pass spinning, and the forming mechanism is complex. The setting of spinning process parameters has a great

influence on the forming quality of the workpiece and the possible defects. The existing research on deep cylindrical parts with a large diameter–thickness ratio was carried out through experiments, but it is difficult to analyze the forming process in detail. The research on deep cylinder parts by finite element simulation is generally limited to the initial few passes, and less research has been carried out on the influence of the process parameters on the spinning force and final forming quality after complete spinning into deep cylinder parts. In this paper, the ten-pass deep drawing spinning process is innovatively adopted. The processing technology of deep cylinders with a large diameter–thickness ratio is simulated. Through experiments, the deep cylinder with a diameter of 500 mm, thickness of 2 mm and depth of 700 mm is successfully spun. Based on the MSC Simufact Forming v16.0 simulation software, after completing the whole pass spinning simulation of thin-walled deep cylinder parts, the influence of mandrel speed, feed rate, spinning wheel fillet radius and spinning wheel angle of attack on the forming spinning force and final forming quality is obtained by a single factor variable analysis method. The results of this paper provide some reference value for the spinning forming process of deep cylinder parts.

2. Finite Element Model and Feasibility Analysis of Deep Cylinder Spinning

Figure 1a shows the part drawing of the deep cylinder. The thickness of the bottom, i.e., the thickness of the blank, is 5 mm, the thinnest part of the cylinder is 2 mm, and the diameter is 526 mm. The deep cylinder is made of 3103 aluminum alloy as a whole, which is formed by the multi-pass spinning drawing process. The feed path of the spinning wheel is shown in Figure 1b. The sheet blank is spun into a deep cylinder after ten passes of spinning.

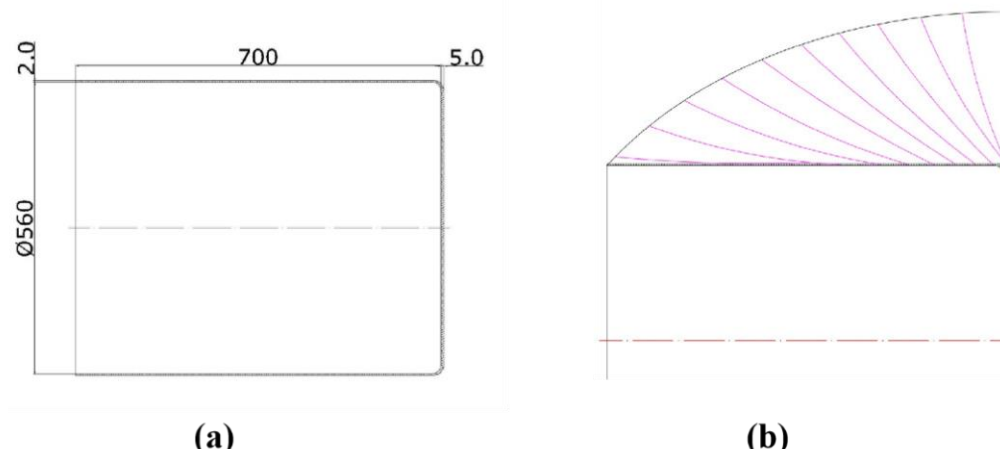


Figure 1. (a) Part sketch of finished deep cup (unit: mm); (b) spinning wheel trajectory.

2.1. Model

Figure 2 shows the finite element model of the multi-pass spinning deep drawing of deep cylindrical parts. The model is mainly composed of the following four parts: tail stock, spinning wheel, blank and mandrel. The blank is fixed at the top of the mandrel under the action of the tail stock. The mandrel rotates at a constant speed and drives the blank to rotate. The spinning wheel moves according to the spinning trajectory shown in Figure 1b, exerting pressure on the blank. At the same time, driven by the blank, the spinning wheel passively rotates to encourage the blank to form towards the target part. In order to speed up the finite element simulation, the size of the model is reduced to a quarter of the original size.

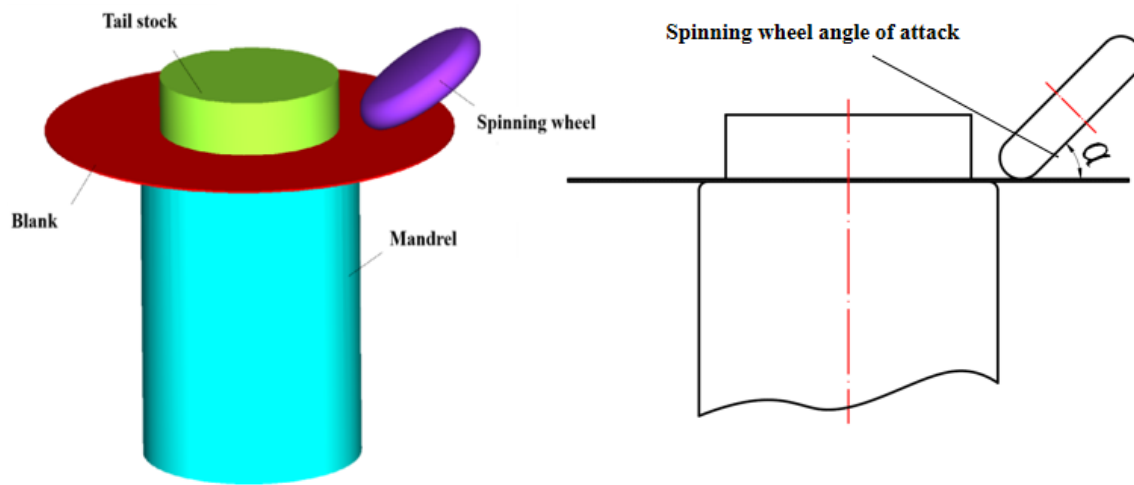


Figure 2. Spinning finite element model.

The blank adopts the 3103 aluminum alloy, which has good elongation, corrosion resistance and processing performance. The flow curve is shown in Figure 3. Obtained via the simufact material library, some of its performance parameters are shown in Table 1. The mesh generator of the blank adopts Sheetmesh, the unit type is hexahedron, the number of units in the thickness direction is set to 3, and the total number of units is 18,927.

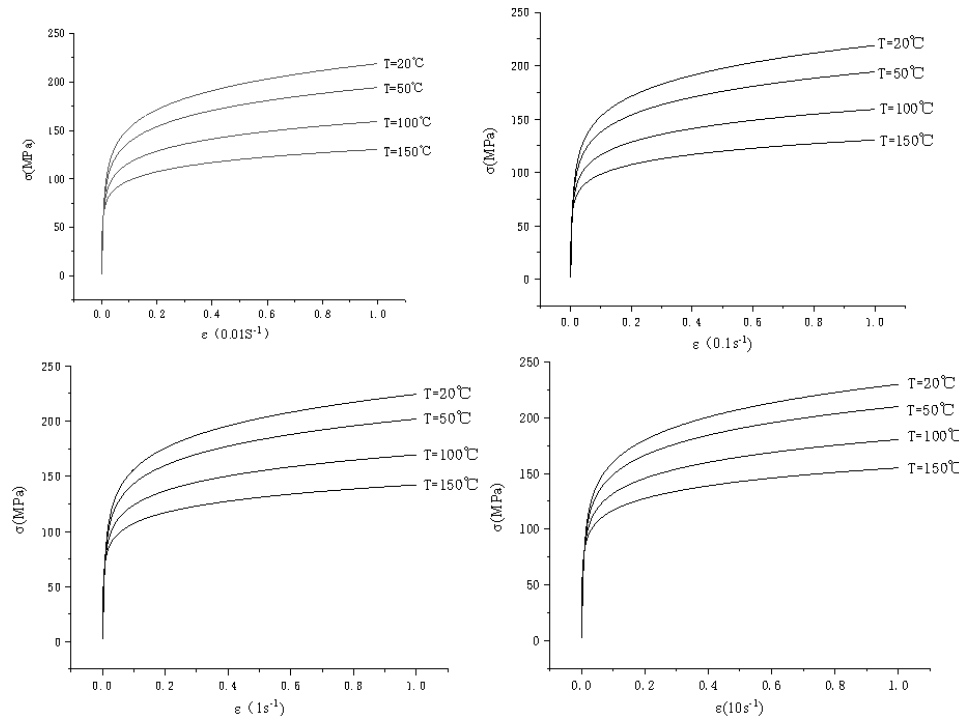


Figure 3. Flow curve of 3103 aluminum alloy.

Table 1. 3103 aluminum alloy material performance parameters.

Parameters	Young's Modulus (E/GPa) (20 °C)	Poisson's Ratio	Yield Strength σ (MPa)	Density ρ (Kg·mm⁻³)
Number	69	0.25	130.111	2725

In the model, the mandrel, tail stock and the spinning wheel are defined as rigid bodies. The contact type of blank and tail stock is defined as glued, and the contact type of

the blank, mandrel and spinning wheel is defined as touching. The friction type between the spinning wheel and the blank is defined as shear friction. Since lubricants are usually added to reduce friction during the actual spinning process, the interface friction factor is set to 0.1. The processing is carried out at room temperature, so the initial temperature of the blank is set to 20 °C, and the ambient temperature is 20 °C. The mandrel, tail block and spinning wheel are defined as constant temperature rigid bodies, and their temperatures are defined as 20 °C. The heat transfer coefficient of all components of the model to the environment is set to 0.05 kw/(m².k), and the thermal emissivity of the environment is set to automatic mode.

2.2. Feasibility and Verification of the Model

After ten passes of spinning, the final forming effect of the blank and the stress–strain diagram of the formed part can be observed, as shown in Figure 4. It can be observed from the figure that the overall deformation of the deep cylinder is uniform and there is no stress concentration. The process of forming deep cylinder parts by spinning is realized by simulation. After parameter optimization, the formed workpiece has uniform strain and no stress concentration. According to the simulation, the ten-pass spinning forming process of deep cylinders is feasible.

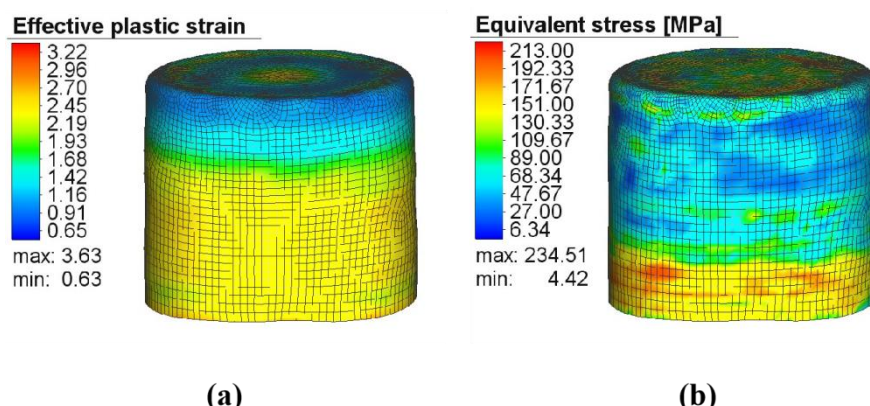


Figure 4. The final formed deep cylindrical parts: (a) equivalent plastic strain diagram; (b) equivalent stress diagram.

In order to verify the feasibility of the simulation results, the spinning process of deep cylinder parts is experimentally explored. The spinning process parameters are shown in Table 2. Figure 5a is the final formed deep cylinder. In order to facilitate the measurement of wall thickness at different positions of the workpiece, it is cut open, as shown in Figure 5b.

Table 2. Process parameters of spinning.

Parameters	Mandrel Speed (rpm)	Feed Rate (f) (mm/rev)	The Spinning Wheel Angle of Attack (°)	The Fillet Radius of the Spinning Wheel (mm)
Number	300	3	30°	9

We measured the wall thickness at different positions of the split deep tube and compared the results with the simulation results. Figure 6 shows that the change trend of the thickness of the deep cylinder after spinning is almost the same as that of the simulation results, and the average wall thickness deviation is 0.5 mm. The part has a large bottom thickness and the side wall gradually becomes smaller. There is evidence of metal accumulation at the mouth of the workpiece, and the wall thickness of the workpiece mouth is greater than the thickness of the blank, which has the effect of spinning thickening

and strengthening the original fragile mouth position. By comparing the wall thickness of the simulation and the test pieces at different positions, the wall thickness trends of the two are almost the same. Because the outermost surface of the workpiece is polished, the wall thickness of the experimental sample is smaller than that of the simulation sample. The experimental results are in line with our expectations, which verifies the accuracy of the spinning model.

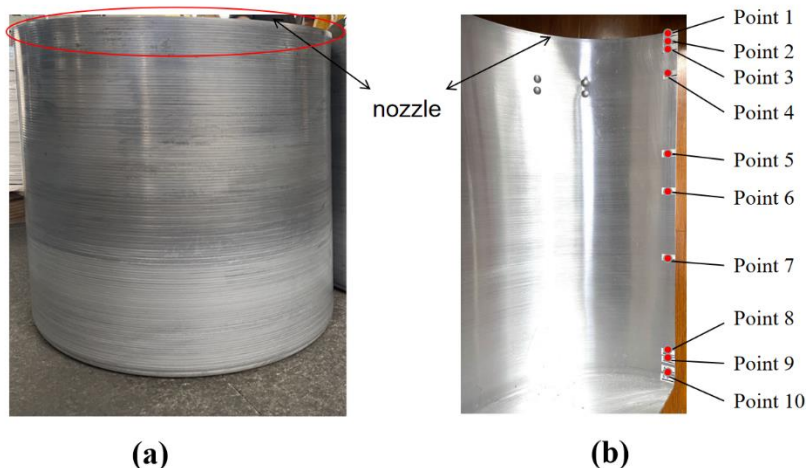


Figure 5. Experiment piece: (a) finished workpiece; (b) sectional wall thickness diagram.

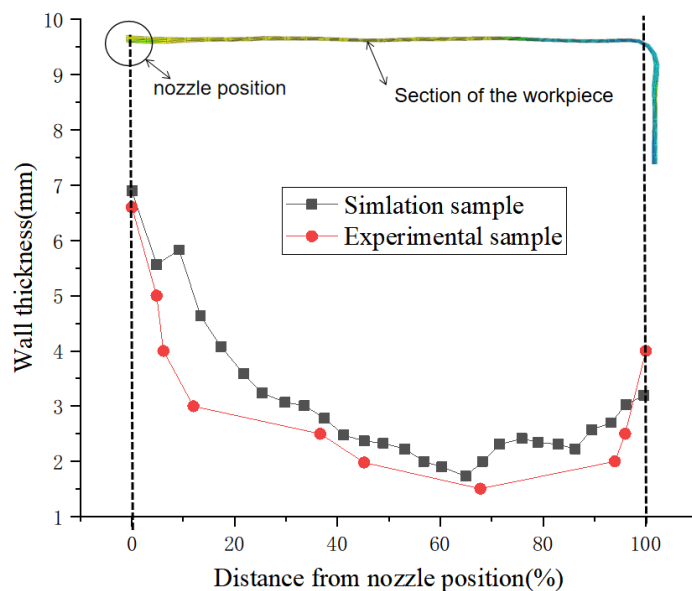


Figure 6. Comparison of the wall thickness data between the simulation and experimental parts.

3. Simulation Results and Analysis

In the process of multi-pass spinning of deep cylindrical parts, the radial spinning force plays the role of pressing the workpiece to make the workpiece stick to the die, and the axial spinning force produces tensile stress on the workpiece along the direction of the spinning wheel. When the axial spinning force is too large, this will cause the workpiece to crack, and a too large tangential spinning force is an important reason for the instability of the workpiece wrinkling. Therefore, under the premise that the spinning can be carried out smoothly, target spinning effect with the minimum spinning force can be achieved. In this paper, the single factor control method is used to simulate the forming process of deep cylinder parts under different parameter levels. The effects of the mandrel speed, the

spinning wheel feed rate, spinning wheel fillet radius and spinning wheel angle of attack on the spinning force and wall thickness deviation are investigated, respectively.

3.1. Effect of Process Parameters on Spinning Force

3.1.1. Mandrel Speed

It can be observed from Figure 7 that in the single-pass spinning process of the deep cylinder, the spinning force generated by the roller is the largest, the axial spinning force is the second largest, and the tangential spinning force is the smallest. When the rotation speed of the roller is 500 rpm, the spinning force is the smallest and the workpiece quality is the best.

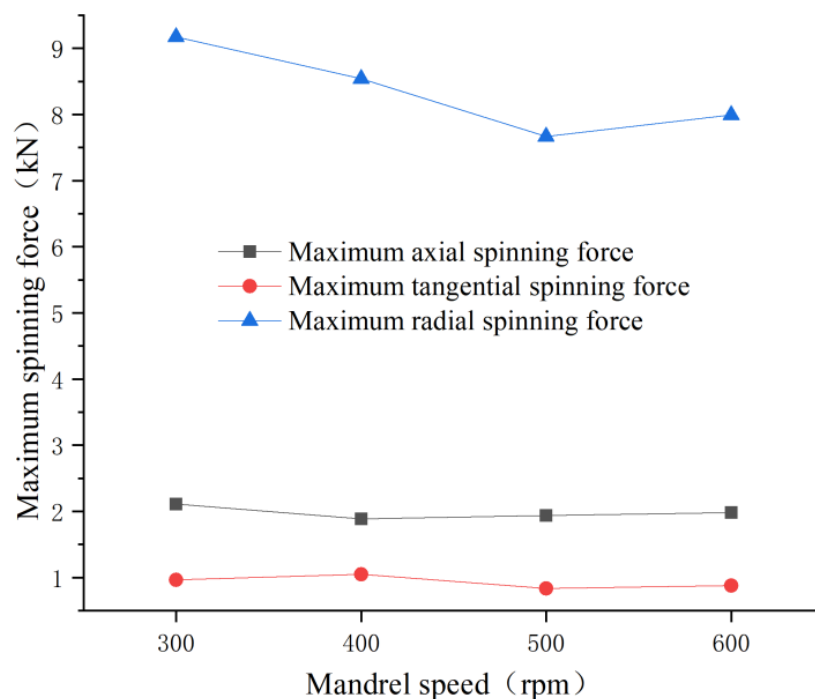


Figure 7. Effect of mandrel speed on spinning force.

By controlling the rotational speed of the mandrel to 300 rpm, 400 rpm, 500 rpm and 600 rpm, it can be observed that with the increase in the mandrel speed, the radial spinning force decreases first and then increases. When the mandrel speed is 500 rpm, both the radial and tangential spinning force are minimized. It can be observed that when the mandrel speed is 500 rpm, the workpiece is the least prone to wrinkling instability. The mandrel speed has little effect on the axial spinning force. When the mandrel speed is 400 rpm, the tensile stress of the roller on the workpiece is the smallest, and the defect of cracking is the least likely to occur. Then, with the increase in the rotational speed, the axial spinning force tends to increase.

3.1.2. Feed Rate

Figure 8 shows the influence of the feed rate on the spinning force. It can be observed that the radial spinning force increases with the increase in the feed rate. Therefore, a relatively small feed rate should be selected when the spinning process has been successfully completed.

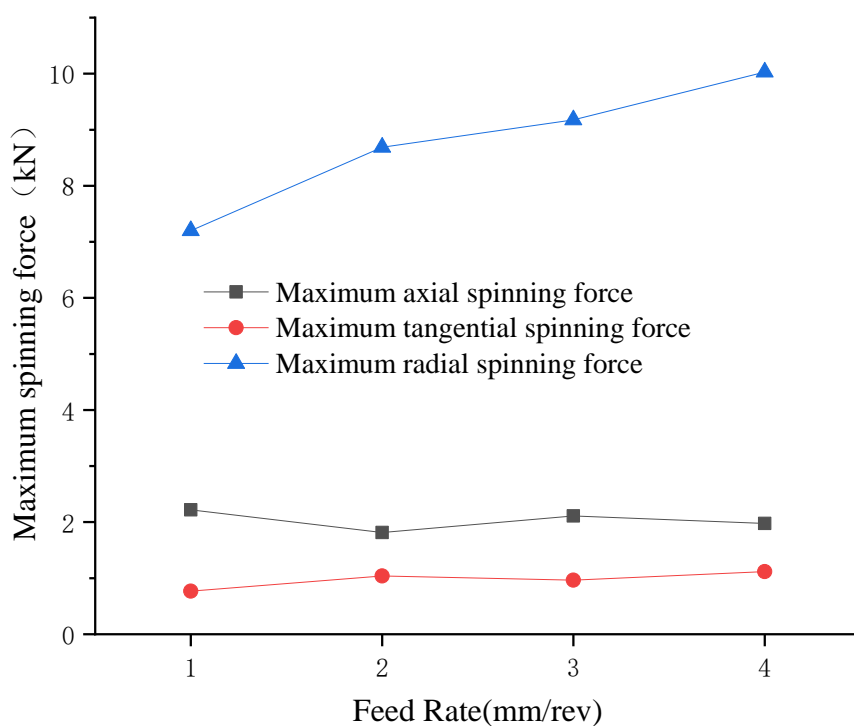


Figure 8. Effect of feed rate on spinning force.

The axial spinning force shows a trend of increasing first and then decreasing during spinning. When the feed rate is 2 mm/rev, the axial spinning force is at its minimum, 1.814 kN, while the maximum value is 2.111 kN when the feed rate is 3 mm/rev. At this time, the workpiece should be prevented from cracking. The tangential spinning force decreases first and then increases. When the feed rate is 3 mm/rev, the tangential spinning force is the smallest and the workpiece is the most stable. At this time, increasing the feed rate will increase the spinning force, which may cause instability and wrinkling.

3.1.3. Spinning Wheel Fillet Radius

In the spinning process, the smaller the spinning wheel fillet radius is, the smaller the overall spinning force is. However, the stress on the workpiece will increase. The spinning wheel fillet radius selected in this paper is 6 mm.

It can be observed from Figure 9 that by changing the process parameters of the spinning wheel fillet radius, the spinning force will be affected as follows. The radial spinning force is the smallest when the radius of the roller is 6 mm and the largest when the radius is 15 mm; when the fillet radius increased to 12 mm, the radial spinning force decreased slightly, showing an overall upward trend. The corresponding axial spinning force also showed the same trend; therefore, in the spinning process, reducing the spinning force may be appropriate for a relatively small roller fillet radius. The tangential spinning force reaches its minimum when the fillet radius of the roller is 9 mm. If the fillet radius continues to increase, the tangential spinning force also increases accordingly, increasing the risk of workpiece instability and wrinkling.

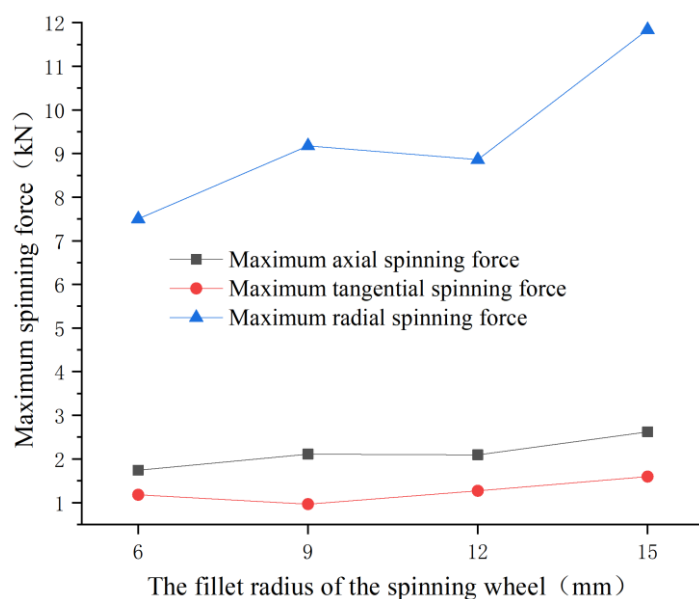


Figure 9. Effect of roller fillet radius on spinning force.

3.1.4. Wheel Installation Angle

It can be observed from Figure 10 that by changing the spinning wheel angle of attack, the three spinning forces show the same trend. As the spinning wheel angle of attack increases, the spinning force increases first, then decreases, and finally increases. When the spinning wheel angle of attack is 35° , the axial spinning force, tangential spinning force and radial spinning force are at their minimum. At this time, the equivalent spinning force is the smallest, and the workpiece is stable and is not prone to instability wrinkling or cracking defects.

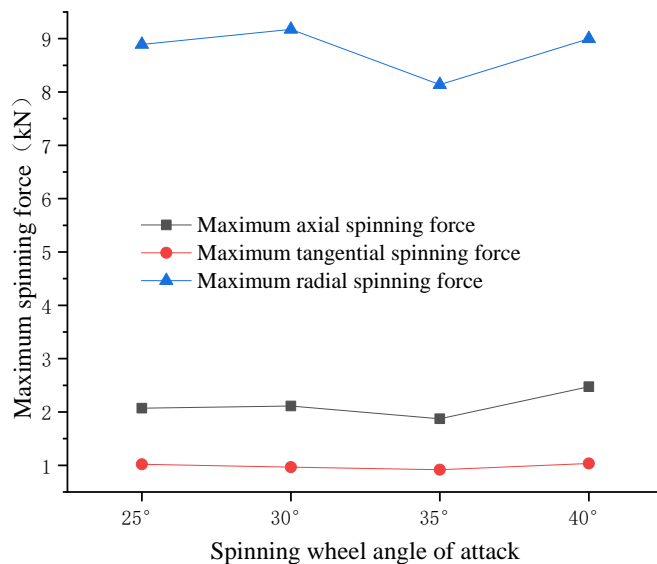


Figure 10. Influence of spinning wheel angle of attack on spinning force.

3.1.5. Instability and Wrinkling Phenomenon

Figure 11 shows the simulation parts with a feed rate of 3 mm/rev and 4 mm/rev. It can be observed from the diagram that the formed parts have different levels of wrinkling. Compared with Figure 11a, when the feed rate is 4 mm/rev, the outer wall and inner wall of the formed part have larger wrinkles. From Figure 8, we also find that the spinning force is the largest at this time.

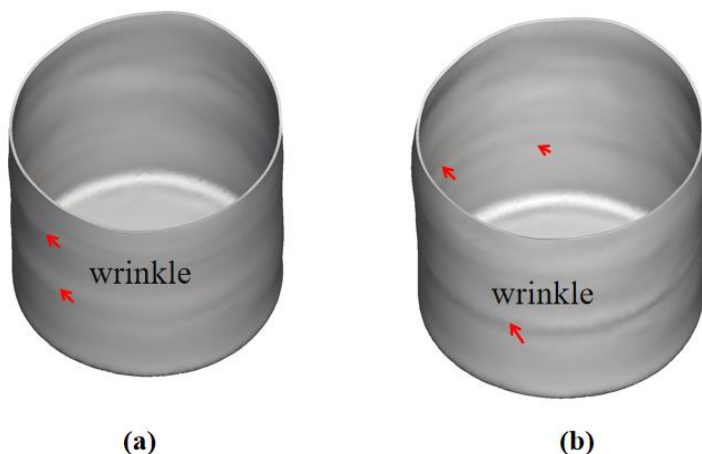


Figure 11. The influence of feed rate on the wrinkling phenomenon: (a) $f = 3 \text{ mm/rev}$; (b) $f = 4 \text{ mm/rev}$.

The circular blank is prone to edge wrinkling during spinning, that is, the edge of the blank is wavy. The instability wrinkling is related to the initial thickness of the circular blank. The thinner the blank and the larger the diameter, the lower the bending stiffness of the workpiece edge. As shown in Figure 12, the reduction in the first pass is too large, resulting in a serious skirt phenomenon. The change trend of each spinning force is shown in Figure 13. Spinning instability starts from about 0.5 s, and the value of each spinning force rises rapidly. In order to prevent the occurrence of this defect, attention should be paid to the reduction in the first pass when designing the roller trajectory. If the reduction is too large, this causes severe wrinkling. At the same time, in the setting of process parameters, defects can be controlled by reducing the feed rate of the roller and reducing the fillet radius of the spinning wheel.

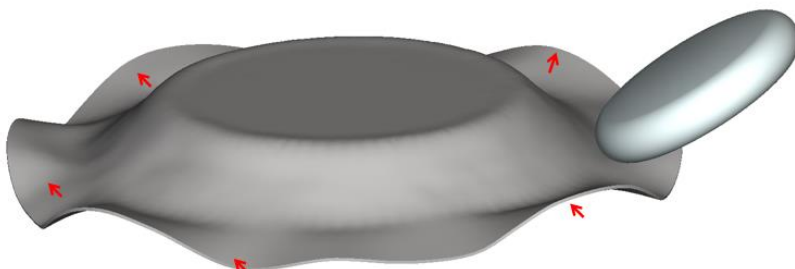


Figure 12. Edge wrinkling phenomenon.

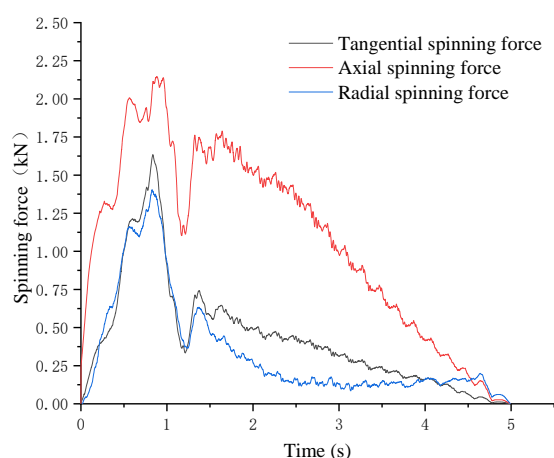


Figure 13. The change trend of spinning force under the condition of instability wrinkling.

3.2. Effect of Process Parameters on Wall Thickness Deviation

Along the axis direction of the deep cylinder parts, 20 sections are taken evenly, and 8 points are taken evenly on each section. The average wall thickness is taken as the wall thickness under the process parameters, and the absolute value of the final wall thickness deviation of the deep tube under each factor level is obtained, as shown in Figure 14. It can be observed that the roller fillet radius has the greatest influence on the wall thickness deviation, followed by the mandrel speed, and then the spinning wheel angle of attack and feed rate.

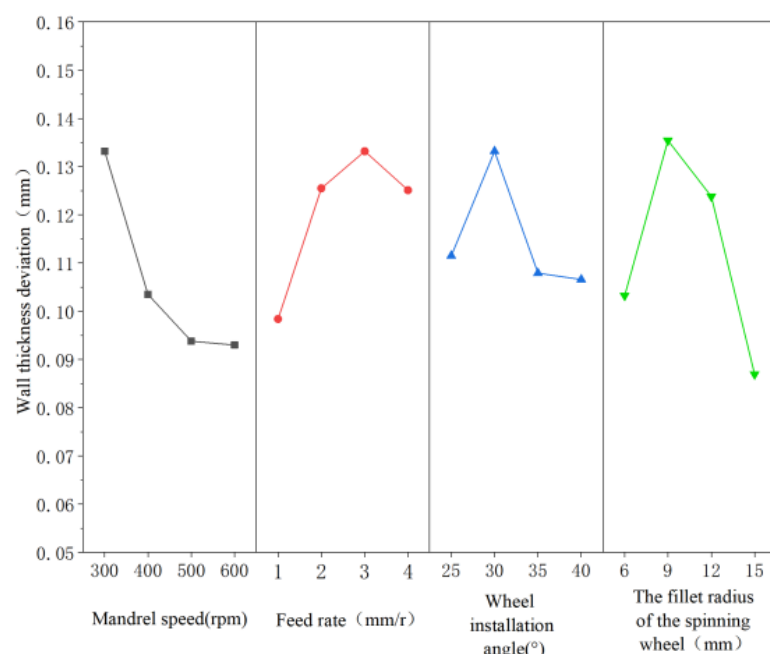


Figure 14. Effect of process parameters on wall thickness deviation.

With the increase in mandrel speed, the wall thickness deviation of the workpiece decreases, and the decreasing amplitude gradually decreases. When the mandrel speed reaches 500 rpm, the wall thickness deviation tends to be stable. With the increase in the feed rate, the deviation of wall thickness increases first and then decreases. When the feed rate is 3 mm/rev, the deviation of wall thickness is the largest. The smaller the deviation of wall thickness, the closer the wall thickness of the spinning part to the theoretical wall thickness and the better the spinning effect. With the increase in the spinning wheel angle of attack and the fillet radius of the roller, the variation trend of the wall thickness deviation is similar, which also increases first and then decreases. When the spinning wheel angle of attack increases to 35°, the wall thickness deviation greatly decreases, and then the decreasing trend is not obvious. When the fillet radius of the roller is 6 mm, the wall thickness deviation is the smallest and the workpiece spinning effect is at its optimum.

4. Conclusions

- (1) Under the influence of different process parameters and different levels, the radial spinning force and the tangential spinning force maintain the same trend. When the mandrel speed, feed rate, roller fillet radius and spinning wheel angle of attack are 500 rpm, 1 mm/rev, 6 mm and 35°, respectively, the radial spinning force and the tangential spinning force are the smallest. At this time, the spinning efficiency is the highest and the workpiece is not prone to defects. If the single-pass reduction is too large, the workpiece is prone to instability and wrinkling. A reasonable reduction will increase the stability of spinning.

- (2) The wall thickness deviation of the workpiece decreases with the increase in the mandrel speed. With the increase in the feed rate, the wall thickness deviation increases first and then decreases. With the increase in the roller fillet radius, the wall thickness deviation increases first and then decreases. With the increase in the spinning wheel angle of attack, the wall thickness deviation increases first and then decreases. When spinning with the process parameters obtained under the minimum spinning force of Conclusion 1, the wall thickness deviation of the workpiece is also small, indicating that the wall thickness deviation of the workpiece is closely related to the spinning force.

Author Contributions: Conceptualization, L.L., Q.L. and X.S.; methodology, L.L., S.C., X.S., Q.L. and J.Z.; software, S.C., Q.L. and W.S.; validation, L.L., S.C. and W.S.; formal analysis, Q.L., X.S. and J.Z.; data curation, S.C. and Q.L.; writing—original draft preparation, L.L., S.C. and Q.L.; writing—review and editing, X.S.; visualization, Q.L. and W.S.; supervision, J.Z.; project administration, X.S. and J.Z.; funding acquisition, X.S. and J.Z. All authors have read and agreed to the published version of the manuscript.

Funding: This study was funded by the Natural Science Foundation of Zhejiang, China (Grant Number: LZ22E050002), the National Natural Science Foundation of China (Grant Number: 51975301), and the Major Project of Science and Technology Innovation 2025 in Ningbo City, China (Grant Number: 2022Z064, 2022Z002), and the Scientific Research Foundation of Graduate School of Ningbo University (No. IF2022097).

Data Availability Statement: Data is contained within the article.

Conflicts of Interest: The authors declare no conflict of interest.

References

1. Yang, Y. *Simulation Study on Power Spinning Dynamics of Cylindrical Parts*; Changchun University of Science and Technology: Changchun, China, 2014.
2. Lu, L. Numerical Simulation of Spinning Forming of Elliptical Tube Shaped Parts based on Deform. *Mod. Manuf. Technol. Equip.* **2016**, *8*, 53–55+82.
3. Lu, Y.L.; Wang, H.Q. Numerical Simulation on Spinning Manufacturing for 1060 Aluminum Alloy Cylinder Part. *Mach. Tool Hydraul.* **2018**, *46*, 39–42.
4. Wang, X.X.; Zhan, M.; Guo, J.; Zhao, B. Evaluating the Applicability of GTN Damage Model in Forward Tube Spinning of Aluminum Alloy. *Metals* **2016**, *6*, 136. [[CrossRef](#)]
5. Shi, L.; Xiao, H.; Xia, Q.X. Study on Forming Mechanism of DP600 High Strength Steel Multi-pass Deep Drawing Spinning. In Proceedings of the 11th China Iron and Steel Annual Conference, Beijing, China, 21–22 September 2017; pp. 48–53.
6. Li, F.G.; Yuan, X.; Hao, X.H.; Liu, T.; Wang, M.J. Influence of the number of power spinning wheels on forming quality for cylindrical parts based on Simufact. *Forg. Stamp. Technol.* **2019**, *44*, 86–91.
7. Zeng, C.; Zhang, S.J.; Xia, Q.X.; Xie, H.X. Research on effect of roller-races and process parameters on multi-pass drawing spinning quality. *Forg. Stamp. Technol.* **2014**, *39*, 58–63.
8. Mei, Y.; Liu, B.; Niu, Z.B.; Zhang, C. Analysis of Forward Spinning for Aluminium Alloy Tube. *Adv. Mater. Res.* **2011**, *1336*, 295–297. [[CrossRef](#)]
9. Zhang, T.; Li, X.H.; Wei, Z.; Chang, S.W. Influence of process parameters on the flow forming quality of thin-walled tube with large diameter-thickness ratio. *J. Plast. Eng.* **2017**, *24*, 75–81.
10. Zhang, H.P.; Ouyang, Z.G.; Li, L.; Ma, W.; Liu, Y.; Chen, F.H.; Xiao, X.H. Numerical Study on Welding Residual Stress Distribution of Corrugated Steel Webs. *Metals* **2022**, *12*, 1831. [[CrossRef](#)]
11. Ma, Z.P.; Li, Y.; Sun, C.G.; Yu, D.T.; Hu, J.Z. Influence analysis of conventional spinning pass curve on forming. *Forg. Stamp. Technol.* **1999**, *24*, 21–24.
12. Pan, G.J.; Li, Y.; Wang, J.; Lu, G.D. Review of conventional spinning process and its roller path design development. *J. Zhejiang Univ.* **2015**, *49*, 644–654.
13. Li, X.B.; Han, Z.R.; Gao, T.J.; Liu, B.M.; Jia, Z. Finite element simulation of multi-pass spinning forming of large complex thin-wall cylinder. *J. Shenyang Aerosp. Univ.* **2016**, *33*, 32–37.
14. Wang, L.; Long, H. A study of effects of roller path profiles on tool forces and part wall thickness variation in conventional metal spinning. *J. Mater. Process. Technol.* **2011**, *211*, 2140–2151. [[CrossRef](#)]
15. Chen, J.; Wan, M.; Li, W.D.; Xu, C.X.; Xu, X.D.; Huang, Z.B. Design of the involute trace of multi-pass conventional spinning and application in numerical simulation. *J. Plast. Eng.* **2008**, *15*, 53–57.
16. He, J.C.; Zhu, S.P.; Luo, C.; Niu, X.; Wang, Q. Size effect in fatigue modelling of defective materials: Application of the calibrated weakest-link theory. *Int. J. Fatigue* **2022**, *165*, 107213. [[CrossRef](#)]

17. Liang, L.; Xu, M.; Chen, Y.; Zhang, T.; Tong, W.; Liu, H.; Wang, H.; Li, H. Effect of welding thermal treatment on the microstructure and mechanical properties of nickel-based superalloy fabricated by selective laser melting. *Mater. Sci. Eng. A* **2021**, *819*, 141507. [[CrossRef](#)]
18. Han, Z.R.; Li, L.; Xiao, Y.; Jia, Z. Effect of feed rate on wall thickness distribution in multi-pass deep drawing spinning. *Light Alloy. Fabr. Technol.* **2019**, *47*, 67–71.
19. He, Q.Z.; Li, H.; Zhao, L.D. Research on dimensional accuracy of multi-step ironing based on Simufact. *Forg. Stamp. Technol.* **2018**, *43*, 108–112.
20. Li, X.M.; Xiao, S.H. Experimental research on one-step drawing and spinning of thin-walled cup. *Die Mould. Ind.* **2014**, *40*, 46–50.
21. Ebrahimi, M.; Tabei, K.H.; Naseri, R.; Djavanroodi, F. Effect of flow-forming parameters on surface quality, geometrical precision and mechanical properties of titanium tube. *Proc. Inst. Mech. Eng. Part E J. Process Mech. Eng.* **2018**, *232*, 702–708. [[CrossRef](#)]
22. Molladavoudi, H.R.; Djavanroodi, F. Experimental study of thickness reduction effects on mechanical properties and spinning accuracy of aluminum 7075 during flow forming. *The Int. J. Adv. Manuf. Technol.* **2011**, *52*, 949–957. [[CrossRef](#)]
23. Wang, D.L.; Guo, Y.M.; Li, Y.N.; Huang, T.; Gao, W.L.; Zheng, H.W.; Xu, H.Q. Numerical simulation and forming precision analysis on counter-roller spinning for large thin-walled cylindrical parts. *Forg. Stamp. Technol.* **2020**, *45*, 47–55.
24. Dahms, F.; Homberg, W. Manufacture of Defined Residual Stress Distributions in the Friction-Spinning Process. Investigations and Run-to-Run Predictive Control. *Metals* **2022**, *12*, 158. [[CrossRef](#)]
25. Du, F.; Xia, Q.X.; Xiao, H.; Shi, L. Analysis on forming quality of high strength steel DP600 cup-shaped part during single-pass deep drawing spinning. *Forg. Stamp. Technol.* **2017**, *42*, 54–59.
26. Gao, S.; Zhao, J.S.; Li, Z.W.; Gao, C.; Li, X.C.; Xie, R. Study on forming accuracy of hot power spinning connecting rod bushing based on Simufact. *J. Plast. Eng.* **2020**, *27*, 40–47.
27. Tang, C.Y.; Fan, W.X.; Yin, X.Y. Forming quality study of power backspinning connecting rod bushing under different rotating wheel parameters based on Simufact. *J. Plast. Eng.* **2018**, *25*, 102–107.

Disclaimer/Publisher's Note: The statements, opinions and data contained in all publications are solely those of the individual author(s) and contributor(s) and not of MDPI and/or the editor(s). MDPI and/or the editor(s) disclaim responsibility for any injury to people or property resulting from any ideas, methods, instructions or products referred to in the content.